Colloids and Surfaces B: Biointerfaces 172 (2018) 280–287

Contents lists available at ScienceDirect

Colloids and Surfaces B: Biointerfaces

journal homepage: www.elsevier.com/locate/colsurfb

Modeling *Escherichia coli* and *Rhodococcus erythropolis* transport through wettable and water repellent porous media

Nasrollah Sepehrnia[a,b,*], Jörg Bachmann[b], Mohammad Ali Hajabbasi[a], Majid Afyuni[a], Marcus Andreas Horn[c]

[a] Department of Soil Science, College of Agriculture, Isfahan University of Technology, Isfahan 84156-83111, Iran
[b] Institute of Soil Science, Leibniz Universität Hannover, Herrenhäuser Str. 2, D-30419 Hannover, Germany
[c] Institute of Microbiology, Leibniz Universität Hannover, Herrenhäuser Str. 2, D-30419 Hannover, Germany

ARTICLE INFO

Keywords:
Bacteria transport
Deposition
Unsaturated flow
Water repellent sand
Hydrophobic bacteria

ABSTRACT

Water protection and bioremediation strategies in the vadose zone require understanding the factors controlling bacterial transport for different hydraulic conditions. Breakthrough experiments were made in two different flow conditions: i) an initial bacteria pulse under ponded infiltration into dry sand (−15,000 cm); ii) a second bacteria pulse into the same columns during subsequent infiltration in constant water content and steady-state flow. *Escherichia coli* (*E. coli*) and *Rhodococcus erythropolis* (*R. erythropolis*) were used to represent hydrophilic and hydrophobic bacteria, respectively. Equilibrium and attachment/detachment models were tested to fit bromide (Br^-) and bacteria transport data using HYDRUS-1D. Derjaguin-Landau-Verwey-Overbeek (DLVO) and extended DVLO (XDLVO) interaction energy profiles were calculated to predict bacteria sorption at particles. Adsorption of bacteria at air-water interfaces was estimated by a hydrophobic force approach. Results suggested greater retention of bacteria in water repellent sand compared with wettable sand. Inverse parameter optimization suggested that physico-chemical attachment of both *E. coli* and *R. erythropolis* was thousands of times lower in wettable than repellant sand and straining was 10-fold lower in *E. coli* for wettable vs repellant sand compared to the exact opposite by orders of magnitude with *R. erythropolis*. HYDRUS did not provide a clear priority of importance of solid-water or air-water interfaces in bacteria retention. Optimized model parameters did not show a clear relation to the (X)DLVO adsorption energies. This illustrated the ambivalence of (X)DLVO to predict bacterial attachment at solid soil particles of different wetting properties. Simultaneous analysis of mass recovery, numerical modeling, and interaction energy profiles thus suggested irreversible straining due to bacteria sizing as dominant compared to attachment to liquid-solid or liquid-air interfaces. Further studies are needed to distinguish straining mechanisms (i.e. pore structure or film straining) in different hydraulic conditions.

1. Introduction

Bacterial transport in soil and aquifers is a widespread problem and has always been important to researchers because of diseases related to human health or with respect to remediation, distortion, and contaminant degradation [1,2]. Understanding the mechanisms of bacterial transport is of great importance to control soil and water pollution and to implement subsurface bioremediation strategies [3,4].

In most bacterial transport studies, soils are water saturated to the desired degree of interest to establish saturated and/or unsaturated steady-state flow conditions before manures are applied [5,6] or bacteria suspensions are injected [7,8] as a pollution source. However, it has also been important to know the extent to which bacteria will be transported if the initial condition of soil is very dry (i.e. close to air-dryness) as is often found in surface soil layers of arid and semiarid climates. To our knowledge, these conditions are seldom part of the experimental design.

Bacterial transport typically depends on their interaction with pore surfaces. Soil particle interfacial properties are controlled by numerous and often coupled physical, chemical, and microbiological factors [4]. Initially dry conditions are crucial for many applications such as bioaugmentation, because bacteria experience more effective passage from upper to the deeper zones to reach the desired subsurface depth. In this respect soils, when either completely dry or with low water content, exhibit water repellency that results in intensive, irregular, preferential, non-equilibrium flow regimes through soil [9–11].

* Corresponding author at: Institute of Soil Science, Leibniz Universität Hannover, Herrenhäuser Str. 2, D-30419 Hannover, Germany.
E-mail address: sepehrnia@ifbk.uni-hannover.de (N. Sepehrnia).

https://doi.org/10.1016/j.colsurfb.2018.08.044
Received 1 May 2018; Received in revised form 17 August 2018; Accepted 19 August 2018
Available online 21 August 2018

However, the coupled effects of bacterial properties and initial dry conditions of soil in conjunction with water repellency are, at present, rarely characterized, which obscures adequate description of relevant mechanisms and the mathematical framework to model pathogen transport for different spatial scales including the column scale [4].

In saturated systems colloid retention is likely to occur in the smallest regions of the pore space usually formed near grain-to-grain contact domains [7,8,12,13] where local water velocity is low and which are considered stagnation zones (Fig. 1). In unsaturated versus saturated media, additional mechanisms favoring colloid retention occur at the solid-water interfaces (SWI) [8,14] and at air-water interfaces (AWI) [15]. Hence, straining [1,7], film straining [16,17], and adsorption at air-water-solid (AWS) triple points at the intersections of air-water-solid interfaces [5,12] are relevant retention mechanisms in 3-phase systems (Fig. 1). Mathematical models developed from simple (i.e. equilibrium) to chemical and physical non-equilibrium approaches (i.e., Two Kinetics Sites, dual-porosity, and dual-permeability) are also fitted to experimental data to reveal the complexity of microbial transport mechanisms [7]. In comparison to wettable media, higher rates of retention are probable in water repellent sand, not only due to grain-grain contact and AWI adsorption, but also caused by coupled effects of bacteria properties (*i.e.* shape, hydrophobicity, and flocculation) and the specific properties at the triple points of the AWS, including straining effects. For partly saturated systems these effects are expected to be more intensive in water repellent media compared to wettable media due to a typically more heterogeneous and disconnected microscopic soil moisture distribution [18].

In most research concerning soil water repellency in context with solute and colloid transport, studies were mostly qualitative due to the complex behavior of water repellent soils. Moreover, understanding bacterial transport and retention mechanisms in a mechanistic framework has received even less attention in water repellent soil materials [15,16]. Correspondingly, our main objectives were: i) to assess the most probable retention mechanisms for bacteria in a wettable matrix compared with a similar, but water repellent counterpart; ii) to proof these transport parameters for consistency for a wide range of dynamic or stagnant water content and water flux conditions. As a first approach, in the present study we investigated two contrasting bacteria different in size, shape, and hydrophobicity. The overall objective was to identify preferential and unfavorable conditions for bacterial transport in a wide range of natural soil conditions.

2. Materials and methods

2.1. Preparation of the wettable and water repellent sand grains and columns

Pure wettable quartz sand with a particle size distribution of 63.4% fine (63 – 200 μm), 36.3% medium (200 – 630 μm) and 0.30% coarse sand fraction (630 – 2000 μm) was used. The sand particles were washed according to Bolster et al. [19]. The pH was 7.50 and the electrical conductivity (EC) was 0.083 (dS m^{-1}) after washing.

The wettability of the sand particles was modified by mixing with polygalacturonic acid (PGA, Sigma-Aldrich) dissolved in water and 1% NaOH, which converted wettable to water repellent sand [20]. Eight g l^{-1} PGA was sufficient to make the sand particles repellent. For 100 g air-dried sand, the carbon added was 0.18%. Subsequently, the pH and EC were 7.28 and 3.29 (dS m^{-1}), respectively.

Particle surface wettability was measured according to Bachmann et al. [21] by the Sessile Drop Method in terms of contact angles (CA) as 0° and 92.7° (± 4.1°) for wettable and water repellent sand particles, respectively. Surface roughness of both sand materials was also measured using an Optical Interferometer [22]. Fogale Pilot 3D software was used to analyze the data.

The same amount of air-dried material, either as wettable or water repellent sand, were separately poured into six PVC columns (height of 18.2 cm and diameter of 7 cm) with 3 replicates for each material. Bulk density of all twelve columns was fixed at 1.53 g cm^{-3}. The column porosity was 0.42. Saturated hydraulic conductivity, K_s, was measured by a constant water head through sand cores (5 cm inner diameter, 5 cm height) and calculated by Darcy's equation [23].

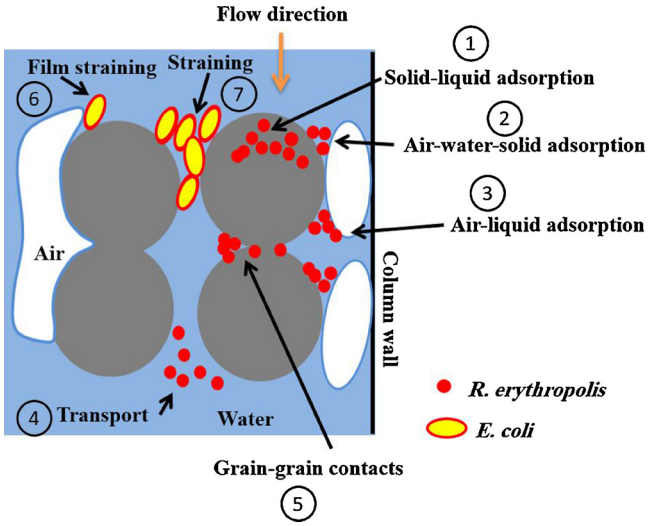

Fig. 1. Schematic figure showing the different retention mechanisms for *Escherichia coli* (*E. coli*) and *Rhodococcus erythropolis* (*R. erythropolis*) in a granular 3 phase system. Figure modified after Zhang et al. [18]. Attachment (k_{att}) and detachment (k_{det}) coefficients, as physcio-chemical and, (film) straining coefficient (k_{str}) as physical retention, are estimated from objects 1 to 4, and, 5 to 7, respectively. The governing equations (attachment/detachment model) for objects 1 to 7 are given in Adamczyk et al. [38], Bradford et al. [7], Schijven and Hassanizadeh [14], Schijven and Šimůnek [36].

2.2. Preparation of bacteria and bromide tracers

Escherichia coli (*E. coli*) as hydrophilic-Gram-negative bacteria and *Rhodococcus erythropolis* (*R. erythropolis,* strain PTCC1767) as hydrophobic Gram-positive bacteria were donated by the Pasteur Institute of Iran, and the Iranian Research Organization for Science and Technology (IROST), respectively. Two suspensions of bacteria with identical concentration were separately prepared and mixed with 10 mM bromide (Br, KBr), a conservative non-reactive tracer. The suspensions had similar chemical conditions (pH, 7.1; EC,1.41 dS m^{-1}) with an influent concentration of 1.00×10^8 CFU ml^{-1} of *E. coli* or *R. erythropolis*. *Escherichia coli* and *R. erythropolis* were cultured on solid Nutrient Agar (NA) for 24 and 48 h, respectively. The 1.00×10^8 CFU ml^{-1} suspension concentration of bacteria cells was prepared on the basis of optical density (OD) measured with a UV–vis spectrophotometer at 518 and 509 nm for *E. coli* and *R. erythropolis*, respectively (Jenway, 6505 scanning spectrophotometer) [19].

2.3. Electrokinetic properties of bacteria cells and sand particles

Bacterial hydrophobicity was measured using microbial adhesion to ultrahydrophobic hydrocarbon testing surfaces (MATH) [24]. The size of bacteria was measured using an optic microscope (Axio Imager. M2, Carl Zeiss). An image processing program (AxioVison, Carl Zeiss) was used to determine the average lengths of the major and minor axes of the cells. At least 100 individual cells were analyzed and the cell size distribution was determined for each organism suspended in 10 mM Br^- at pH 7.0.

A ZetaPALS analyzer (Brookhaven Instruments Crop) was used to characterize the zeta potentials (ζ) of the microorganisms (1.00×10^8 CFU mL^{-1} in 10 mM Br^-) and of the wettable and water repellent sand at 20 °C. These measurements were repeated ten times. Both bacterial

suspensions were prepared from a Nutrient Agar medium culture. The ζ-potential, MATH, size, and shape of bacteria were analyzed before the column experiments.

The interaction energy of *E. coli* and *R. erythropolis* with soil particles were calculated using DLVO (Derjaguin–Landau–Verwey–Overbeek) and the extended DLVO (XDLVO) theory [25,26]. The DLVO interaction energy consists of the sum of attractive van der Waals [27] and repulsive electrostatic double layer interactions [28]. The XDLVO also includes acid-base (AB, hydrophobic forces) interactions [29] to account for H-bonding effects that are not considered by DLVO. Both theories give the solid-bacteria interaction energy in water under the geometrical assumption of spheres (bacteria) and plates (sand particles) [30]. Hydrophobic interaction energy between bacteria and air-water interfaces was estimated according to Yoon et al. [31], because, Hydrus is not able to distinguish between adsorption on grains or on air-interfaces.

2.4. Leaching set up

Transport of *E. coli* and *R. erythropolis* was performed in separate columns under identical conditions. The influent suspensions containing bacteria and Br^- were poured on the top of the columns in two pulses. First, a pulse of bacteria (*E. coli* or *R. erythropolis*, 1.00×10^8 CFU ml^{-1}) equal to 62 ml (equivalent to 0.1 the maximum column pore volume [PV] for a natural wettable soil in saturated flow; data are not presented) was poured on the surfaces of the columns. Directly afterwards, a constant saturated flow condition was applied to the top of columns using a disc infiltrometer. Leaching continued for 4 PVs using tap water (pH, 8.30; EC, 0.40 dS m^{-1}). Next, a second pulse of bacteria (with similar concentration and volume as the first pulse) was poured on the surface of columns. Leaching was thereafter continued until 6 PVs with the background solution. Two extra PVs of leaching were used to see if any bacteria release trend occurred in the second pulse.

2.5. Effluent sampling

Effluent samplings of bacteria and Br^- were done at the bottom outlet of each column. During the first pulse, the effluents were taken at 0.1 PV increments for the first and at 0.25 PV increments for the following three PVs, respectively. Sampling was repeated accordingly for the second pulse (4 PVs to 10 PVs) at the respective time intervals. Small amounts (0.1 ml) of diluted solution were added to EMB (Eosin Methylene Blue, Merck) and NA (Nutrient Agar, Merck) media to recover *E. coli* and *R. erythropolis*, respectively.

To account for entrained bacteria, columns were sliced into increments of 3 cm thickness after leaching. One gram of sand in triplicate from each increment was poured into 9 ml water and agitated using a vortex mixer (VWR International, Germnay) at the rate of 300 rpm to release bacteria from the sand surface [16,33]. One ml of the solution was gathered and diluted using a similar procedure as used for the leachate and the influx concentration of bacteria. The colony forming units (CFUs) of bacteria in the leachates and the sand extracts were counted by the plate-count method and reported as CFU mL^{-1} [34]. Effluent Br^- concentrations were individually analyzed using a bromide-specific electrode (ion selective meter, MP523).

2.6. Modeling procedure

HYDRUS-1D (version 4.16.0110) [35] was used to simulate water flow and breakthrough curves of Br^-, *E. coli,* and *R. erythropolis* using an inverse modeling routine based on the one-dimensional Richards' equation for unsaturated water flow and the convection-dispersion model for solute and colloid flow [35]. For details of model set-up see Supplementary material.

Regarding bacteria transport and sorption, the two kinetic sites model (particle transport using attachment/detachment, chemical nonequilibrium) (Fig. 1) was fitted to the experiment data of *E. coli* and *R. erythropolis* and the simulation was separately done for each bacterial BTC. Attachment (k_{att}) and detachment (k_{det}), coefficients using Langmuirian dynamics and straining (k_{str}) in terms of irreversible straining by using depth dependent blocking coefficients [7] were optimized. An empirical factor controlling the shape of the spatial distribution through the profile (β) was fixed to 0.43 which allowed us to compare the relative importance of straining and attachment [7]. Readers are referred to Adamczyk et al. [38], Bradford et al. [7], and Schijven and Šimůnek [36] for the governing equations.

3. Results and discussion

3.1. Bacterial cell properties

Rhodococcus erythropolis (*R. erythropolis*) had greater negative surface charge (–44.39 ± 1.57, mV) than *Escherichia coli* (*E. coli*) (–33.05 ± 0.99, mV) for the Br− solution (10 mM). For comparison, Schäfer et al. [32] found a ζ-potential of –44.80 mV for *Rhodococcus* sp.*125C*. Interestingly, the surface charges of both bacteria were markedly different ($p < 0.001$) in distilled water (–38.23 ± 1.80 and –68.33 ± 1.23 mV, respectively) if compared with 10 mM Br− data. This result suggested that part of the soluble ions were adsorbed at the cell interfaces and neutralized the surface charges. In general, this can be considered a result of increased compression at the higher ion concentration of the diffuse layer of ions forming the interphase of the cell [39]. *Rhodococcus erythropolis* had greater negative surface charge values for both measurements (distilled water and 10 mM Br−) and values were more affected by the10 mM Br− compared to *E. coli.*

The level of water repellency was also significantly different between bacteria ($p < 0.001$). On average, 11% and 73% cells of *E. coli* and *R. erythropolis,* respectively, were captured at the hydrocarbon surfaces. This demonstrated that the higher negatively charged *R. erythropolis* surfaces were more hydrophobic than the less negatively charged *E. coli* surfaces. Hamadi and Latrache [40] found 0−5% hydrophobicity for *E. coli* measured with hexane. Chang et al. [41] found 68% hydrophobicity within 3 h for *R. erythropolis*. These results indicate that hydrophobicity and ζ-potential are positively correlated for the selected bacteria.

Shape and size of *E. coli* and *R. erythropolis* were significantly different ($p < 0.001$). On average, *E. coli* was longer (2.05 μm) than *R. erythropolis* (1.47 μm). The widths of bacteria (1.2 and 1.1 μm for *E. coli* and *R. erythropolis*, respectively) were approximately similar. Consequently, cell shape factor (Width/Length) showed greater deviations for *E. coli* (0.59 ± 12) from spherical compared to *R. erythropolis* (0.77 ± 0.17). The measurements illustrated that *E. coli* and *R. erythropolis* were best approximated as rod and coccid shapes, respectively.

3.2. Simulation of water flow

Some of the physical and hydraulic properties of the sand column media are presented in Table 1. The residual water content (θ_r), the inverse of the air entry value (α), and the pore size distribution of the soil (n) were estimated from independently measured sand water characteristics curves (SWCC) fitted to the van Genuchten model [37]. These settings were used as fixed parameters for the Br^- and bacteria BTC simulations. This enabled us to reduce the parameters in inverse modeling of hydraulic properties considerably. Next, θ_s, K_s, and l remained to be fixed according to the Br^- transport experiment using the HYDRUS equilibrium model code (Table 1). Accordingly, the predicted hydraulic parameters using HYRDUS (θ_{max}^{**} and K_s^{**}) were more appropriate to simulate bacteria transport and retention in these larger-scaled column systems in ponded infiltration conditions than conventional θ_s and K_s from independent and smaller core samples.

Table 1
Physical and hydraulic properties of the wettable and water repellent sand columns. θ_r: the residual water content, θ_s: the saturated water content, θ_{max}^{*}: the maximum water content measured by weight in the saturated flow condition, θ_{max}^{**}: inversed saturated water content, α: the parameters related to inverse of the air entry value, n: pore size distribution index, K_s and K_s^{**}: observed and inversed saturated hydraulic conductivity, v: pore water velocity, l: tortuosity factor, τ: the imposed flow, V_t: total volume of the columns, PV: pore volume, Pe: Peclet number.

Type of sand	θ_r[a]	θ ($cm^3\ cm^{-3}$)$_s$[a]	θ_{max}^{*}	θ_{max}^{**}	α[a] (cm^{-1})	n[a] (-)	$Ks\ v$ (cm min^{-1})		K_s^{**}	l (-)	τ (cm)	V_t (cm^3)	PV (cm^3)	Pe (-)	R^2
wettable	0.01	0.36	0.34	0.31	0.012	1.83	3.80	11.2	1.29	3.50[b]	0	984	331	135.0	0.97
repellent	0.01	0.39	0.23	0.26	0.012	1.87	1.10	5.00	0.327	2.68[c]	0	984	217	19.0	0.90

[a] and* estimated from sand water characteristic curve by fitting van Genuchten model [40] and measured after leaching, respectively. PV is product of θ_s^{*} in V_t, $Pe = L \times \lambda^{-1}$ (L: length of column, λ: dispersivity).**: inversed from Br^- data using HYDRUS.
[b] (1.64 ± 1.07 and 5.34 ± 0.96 for wettable sand columns treated with *Escherichia coli* and *Rhodococcus erythropolis*, respectively).
[c] (3.30 ± 3.96 and 2.06 ± 1.16 for water repellent sand treated with *Escherichia coli* and *Rhodococcus erythropolis* columns, respectively).

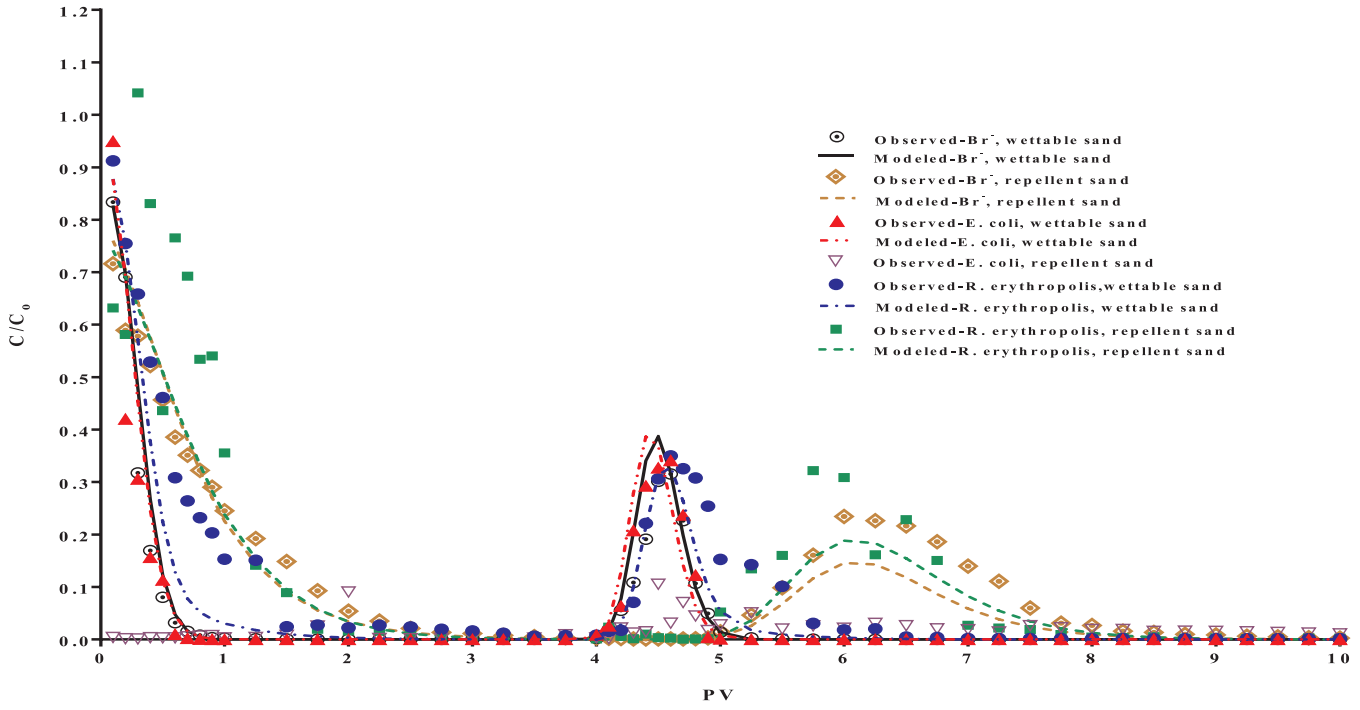

Fig. 2. Observed (symbols) and modeled (lines) breakthrough curves of Bromide (Br^-), *Escherichia coli* (*E. coli*) and *Rhodococcus erythropolis* (*R. erythropolis*) related to the wettable and water repellent sand columns. Data are average of three replicates for each bacterium. *Escherichia coli* fitting was not successful in water repellent sand. Br^- data are average of six replicates (three replicates for each bacterium).

3.3. Observed and fitted bromide transport

Fig. 2 shows observed and simulated (normalized to influx concentrations, C/C_0) Br^- concentrations as a function of PV. Br^- acted as a conservative tracer with a total mass recovery rate (summation of the first and second pulse) representing on average 94% and 86% of the effluent for experiments made in wettable sand with *E. coli* or *R. erythropolis,* respectively and 88% and 80% for experiments in the water repellent columns (Table 2). The lower mass recoveries in water repellent columns might be explained by the higher number of less mobile water domains and physically trapped Br^- solution compared with wettable sand. Mass recovery for each pulse is also given in Table 2.

The peak values of C/C_0 in the first pulses were around 0.7 − 0.9 and reached the end of the columns after 2.70 ± 0.30 min and 8.80 ± 0.60 min as the first arrivals (1 PV) in the Br^- − BTCs for wettable and repellent sand, respectively (Fig.2). The longer duration for first arrivals for the repellent sand indicated that high local hydraulic pressure gradients were needed to infiltrate into the column pathways and to overcome local particle water repellency [9]. Interestingly, the peaks declined to relative values of 0.35 − 0.40 for the second pulses. This indicates Br^- dilution due to increased water content lower in Br^- concentration after the first pulse. This supports the assumption of dual permeability percolation, which may describe the hydraulic situation best during the second infiltration [44]. This also might explain the lower peak concentration in the almost saturated column in comparison with the initially dry conditions in the first pulse injection, because convective and diffusive mixing processes of invading and static residual solution may occur.

The equilibrium model provided an excellent explanation of the wettable and water repellent Br^- − BTCs (Fig. 2) when used for the inverse optimization of the dispersivity λ ($R^2 > 0.90$). Thus, HYDRUS was able to describe initially dry conditions with the same set of parameters. Dispersivities were always considerably higher in water repellent sand compared to wettable sand (Table 3), indicating greater heterogeneity and more dispersive Br^- pathways in repellent conditions. Relatively variable mass balance data (Table 2) for each pulse also illustrated that Br^- experienced a more heterogeneous physical pathways in water repellent sand than wettable sand.

Table 2
Experimental mass balance of *Escherichia coli* (*E. coli*), *Rhodococcus erythropolis* (*R. erythropolis*), and Br^- for the wettable and water repellent sand.

Sand type	Wettable				Repellent			
	Bacteria		Br^-		Bacteria		Br^-	
Mass type	*E. coli*	*R. erythropolis*	Br-E	Br-Rh	*E. coli*	*R. erythropolis*	Br-E	Br-Rh
First -Pulse	70.00 (± 3.60)	81.00 (± 7.10)	86.00 (± 0.38)	66.00 (± 0.50)	6.20 (± 1.40)	93.30 (± 12)	100.00 (± 0.10)	84.30 (± 3.60)
Second-Pulse	129.00 (± 0.36)	94.00 (± 5.60)	96. 00 (± 0.38)	105.00 (± 1.00)	15.20 (± 1.00)	92.00 (± 7.30)	71.00 (± 0.6)	70.00 (± 1.40)
Total effluent	99.00 (± 1.64)	87.00 (± 6.10)	94.00 (± 0.132)	86.00 (± 0.31)	11.00 (± 0.35)	92.40 (± 0.30)	88.40 (± 0.3)	80.00 (± 1.14)
Resident	0.70 (± 0.61)	10.00 (± 0.37)	_	_	77.50 (± 11.20)	8.00 (± 1.30)	_	_
Resident + Effluent	99.70 (± 1.50)	97.00 (± 6.40)	_	_	88.50 (± 4.70)	100.40 (± 1.50)		
Error	−0.30	−3.00	+6.00	−14.00	−11.50	+0.40	+11.60	+20.00

Br-E and Br-Rh indicate the Br^- relevant to the *Escherichia coli* and *Rhodococcus erythropolis* columns. The data are mean values of three replication and figures in parentheses are standard deviation.

Table 3
Transport parameters (Bromide dispersivity λ, straining coefficient k_{str}, attachment coefficient k_{att}, and detachment coefficient k_{det}) fitted using the effluent and the deposition concentrations of bacteria for the wettable and water repellent sand.

Sand	Wettable		Repellent	
parameter	*E. coli*	*R. erythropolis*	*E. coli*[a]	*R. erythropolis*
λ (cm)[b]	0.124 (± 0.01)	0.128 (± 0.01)	0.853 (± 0.21)	0.735 (± 0.45)
k_{str} (min^{-1})	0.204 (± 0.354)	0.11 (± 0.103)	6.97 (± 11)	0.00014 (± 0.0001)
k_{att}(min^{-1})	0.00004 (± .0001)	0.000002 (± 0.000001)	0.152 (± .076)	0.0001
k_{det} (min^{-1})	3.86 (± 6.40)	0.867 (± 0.867)	1.90 (± 3.20)	0.153 (± 0.122)
β	0.43	0.43	0.43	0.43
R^2	0.93	0.95	0.74	0.86

[a] Only the retention (deposition) profile data were successful.
[b] Fitted from bromide data. The data are mean values of three replication and figures in parentheses are standard deviation. β was fixed to 0.43 to compare the relative importance of straining and attachment [6].

3.4. Observed bacteria transport

Similar breakthrough curves were observed for *E. coli* and *R. erythropolis* for the wettable sand (Fig. 2). The heights of peak concentrations of both bacteria strains in the first pulse reached the levels of C_0. In the second pulse, concentrations were roughly reduced to half of input concentration, i.e. $C_0/2$ (Fig. 2). Similar to Br^-, the high concentration in the first peak is the result of dry initial conditions. Closer inspection shows some release (tailing) behavior was more pronounced for the falling branch of *R. erythropolis* BTC after injection of each pulse (Fig. 2). More than 70% and 58% of the injected *E. coli* were recovered in the effluent before 0.5 and 4.5 PVs for the first and second pulse injection; these values were considerably lower for *R. erythropolis* (40% and 25%, respectively). Apparently, a great portion of injected hydrophobic *R. erythropolis* cells were removed initially by adsorption from the solution, and then detached from the retention sites [45]. The effluent recovery of *E. coli* increased from 70% in the first pulse to 129% in the second pulse (Table 2). A similar recovery was also found for *R. erythropolis,* but with a much less significant difference between first and second pulse (81% vs. 94%) supporting greater detachment and remobilization potential of hydrophilic rather than hydrophobic bacteria [45].

For the water repellent sand (Fig. 2) *R. erythropolis* showed more scattering and higher cell concentrations in the out-flux concentration than the initial concentration ($C > C_0$), in particular when the cell effluent appeared early (0.3 PV, Fig. 2). Higher effluent concentrations for *R. erythropolis* before 1 PV could (similar to Br^- transport) be associated with preferential flow pathways [7,35,46], blocking [47], and subsequent detachment [6]. Blocking of the retention sites was unlikely for such zero-initial water content condition at the early stage of leaching. Detachment from the retention sites of water repellent sand was possible according to the hydrophobic tendency of *R. erythropolis* cells as discussed for wettable sand. However, the more likely reason could be preferential transport, because the amount of trapped air was higher in water repellent sand (Table 1) after infiltration. Prolonged water repellency pushes water into larger pores where the lowest hydraulic friction and the lowest water entry pressure, but the highest velocities on the pore scale occur [9]. Such a trend ($C > C_0$) in transport of *R. erythropolis* could be based, in tendency, on preferential (faster) transport because the first arrivals (8.80 ± 0.60 min) were approximately equivalent to one PV (the so called active apparent pore volume). Initial detachment of early attached bacteria due to decreased film straining effects with time [48] along with preferential transport may have caused the observed ($C > C_0$) trend for *R.* erythropolis. Such conditions could also accelerate *E. coli* transport, but here the BTCs suggested high retention for *E. coli* in both pulses (Fig. 2) without initial detachment tendency. The retained mass for *E. coli* was 77.5%, while, it was only 8% for *R. erythropolis*, suggesting different processes in unsaturated soil.

3.5. Observed bacteria retention

The retained concentration profiles of the bacteria (S/C_0) are plotted vs. column depth (0–18 cm) in Fig. 3. Interestingly, the shape of the retention profiles were similar for both bacteria in the wettable sand while corresponding profiles were extremely different in the water repellent columns. It is interesting to note, that similar trends, classified

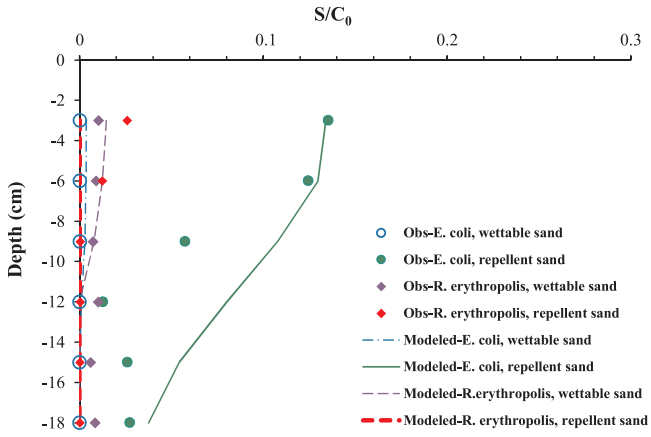

Fig. 3. Measured (symbols) and fitted (lines) *Escherichia coli* (*E. coli*) and *Rhodococcus erythropolis* (*R. erythropolis*) relative concentrations deposited in the wettable (a) and repellent (b) sand columns after termination of the experiment.

as exponential and hyper-exponential trends with depth, were comparable with similar studies made in wettable and water repellent sandy media [8,16,45,48].

Both bacteria were less retained in the wettable sand than the water repellent counterpart. The retention of *R. erythropolis* was slightly higher than for *E. coli* in wettable sand. The trend was reversed in the water repellent sand and more *E. coli* were retained in both pulses (Table 2). The higher removal of bacteria, particularly for the less saturated column (pulse 1, Table 2), was also in accordance with previous studies reported for unsaturated sand columns [2,8,45].

3.6. Bacteria transport modeling

Lines in Fig. 2 illustrate simulated BTCs for *E. coli* and *R. erythropolis* transport. The data are mean values of the BTCs as done in triplicate. *Escherichia coli* retention was high and modeling was only successful for the retention profile as indicated in Fig. 2. Simulation of retention profiles performed generally well for the wettable and the water repellent media (R^2 = 0.74–0.95). The respective parameters of bacterial transport and retention are given in Table 3.

Simulations showed similarity to $Br^- -$BTC higher values for dispersivity in water repellent vs. wettable sand, indicating stronger contrast between regions with higher and lower transport velocity (i.e. caused by the tendency for preferential flow pathways in the water repellent medium along with more trapped air). In comparison, values for dispersivity were similar to other wettable or repellent sand columns studies [7,16].

The differences in the attachment (k_{att}), straining (k_{str}), and detachment (k_{det}) coefficients between the strains were enhanced in the water repellent sand compared to wettable sand. The parameters were robust (Table 3), so that k_{str} dominated compared to k_{att}. This demonstrates the importance of straining relative to attachment, however, it does not mean that attachment was unimportant in this study. For example, the k_{att} values for bacteria in water repellent sand were several orders of magnitude higher than for wettable sand, suggesting the importance of attachment and dependency of retention on porous media wettability. Further, similar values of k_{str} and k_{att} for *R. erythropolis* also indicate the importance of straining and attachment mechanisms in water repellent sand. The results were in accordance with Bai et al. [16] who reported greater k_{str} than k_{att} for hydrophilic *Klebsiella* sp. (i.e. 0.91 vs. 0.31 min^{-1}) compared to hydrophobic *R. rhodochrous* (i.e. 0.64 vs. 0.18 min^{-1}) in a fine sand (i.e. CA = 59.8°). However, they found greater k_{str} coefficient for *R. rhodochrous* (i.e. 0.59 min^{-1}) in a coarse sand (i.e. CA = 35°) in comparison with *Klebsiella* sp. (i.e. 0.00002 min^{-1}).

The detachment coefficients, k_{det}, also showed differences for bacteria transport in the media (Table 3). The rate of bacteria detachment was higher in wettable sand than water repellent sand, i.e. k_{det} coefficients for both bacteria were higher than k_{str} and k_{att}, indicating both reversible attachment and straining in the wettable sand. This was also supported by bacteria mass recovery where more than 80% was found in the sand. For the water repellent sand, although k_{det} coefficients were supported by mass recovery both strains acted differently. The k_{det} was smaller as were k_{str} and k_{att} for *E. coli*, illustrating, in tendency, attachment and straining. For *R. erythropolis*, the k_{str} and k_{att} values were similar in magnitude, but the sum was smaller than the k_{det}, suggesting higher mobility. The k_{det} was higher for *E. coli* compared to *R. erythropolis* in both sandy media, supporting higher detachment of hydrophilic than hydrophobic bacteria in accordance with others [15,19,32].

Inverse simulation gives a coefficient for bacteria attachment including physical adsorption at solid-water and air-water interfaces. The inverse optimization using HYDRUS does not identify relative importance of each mechanism in bacteria retention i.e. if solid-water or air-water contributed more. Similarly, straining includes bacteria filtration as the result of pore structure and film straining. Straining can occur at $d_p/d_g > 0.002$ [7,8], where d_p and d_g are colloid and grain diameters, respectively. This ratio was 0.07 and 0.04 for the longest and the smallest dimensions of *E. coli*. Similarly, 0.05 and 0.04 were calculated for *R. erythropolis* which demonstrates that straining can occur under the conditions of this study. It has been illustrated that bacteria straining will be increased in unsaturated conditions as the result of AWS interface [5,8,48], pore size staining [7,8,19,48], and film straining [18,48]. Assessment of film straining needs further water film thickness calculations [50] which were beyond the scope of this paper.

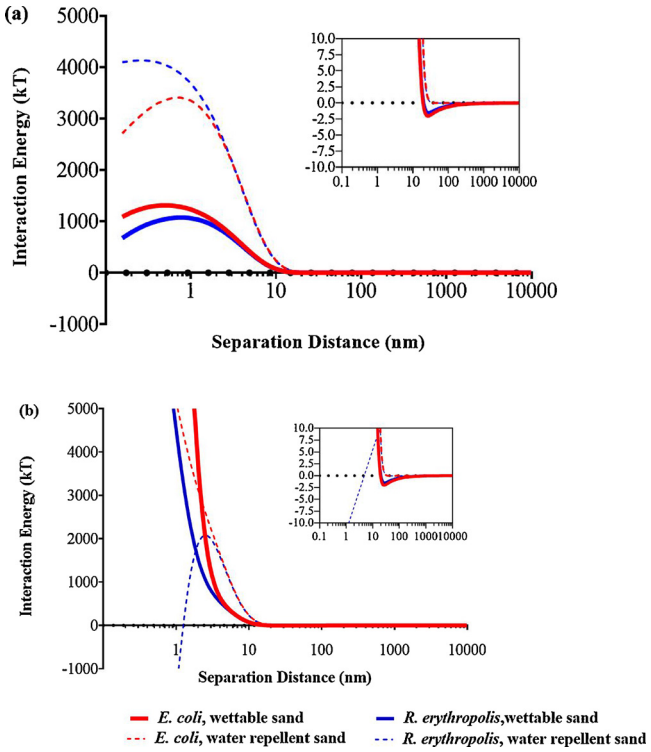

Fig. 4. Calculated DLVO (a) and XDLVO (b) interaction energies for *Escherichia coli* (*E. coli*) and *Rhodococcus erythropolis* (*R. erythropolis*) in the wettable and the water repellent sand. Subgraphs are detailed view of energy barriers and secondary minima.

3.7. Solid-water-air-bacteria cell interaction energies at pore scale

3.7.1. DLVO interactions

The DLVO energies (Fig. 4a) were estimated for bacteria-solid-water and bacteria-air-water interactions. The DLVO showed a secondary but not a primary energy minimum for bacteria-solid-water interfaces for both sand media, This indicated no permanent retention, but possible reversible attachment for bacteria in the secondary minimum [16,49–52]. The values of k_{det} predicted from inverse modelling confirms generally reversible attachment conditions for both bacteria (Table 3).

The DLVO calculations showed unfavourable attachment conditions for strong adsorption in the primary minimum due to high energy barriers for all combinations of bacteria and sands (Fig. 4a). Probable lower energy barriers for bacteria in wettable sand than calculated could be supported by extended surface roughness of the sand particles. The larger surface roughness for the wettable sand (11.10 μm) compared with water repellent sand (4.70 μm) might reduce repulsive energies and favour the tendency for bacteria attachment and retention as reported by Shen et al. [52].

Escherichia coli and *R. erythropolis* exhibited a deeper secondary minimum (2.03 and 1.52 kT, ~28 nm) in the wettable sand compared with the water repellent sand (0.02 kT, at ~45–50 nm), indicating

higher tendency for adsorption [49–52], because a depth of the energy levels equal or deeper than 0.5 kT is greater than the thermal kinetic energy of a bacteria which is the threshold for adsorption in the second minimum [51]. Therefore, only a few bacteria should be held due to the small secondary energy minimum of the water repellent sand. But, interestingly, the water repellent sand showed greater retention of both bacteria compared to the wettable sand. This illustrated the problem of using DLVO to predict bacteria attachment and suggested that bacteria retention might be controlled also by other mechanism(s) in the water repellent sand. Theoretically, attached bacteria in the secondary minimum could experience further impact of hydrodynamic forces (fluid drag, lift forces) caused by water flow, which also supports detachment [8,52]. Experimentally, Shen et al. [52] investigated adsorption at three ionic strengths (1, 200, and 300 mmol L^{-1}) and concluded that the initial attached colloids at the tips of asperities became detached at low ionic strength because destabilizing forces became larger than attractive forces.

Finally, the DLVO profiles showed that attachment is more determined by sand wettability rather than bacteria wettability (Fig. 4a). Taking into account that some bacteria cell walls had a significant degree of hydrophobicity, it can be assumed that bacteria cells are also attracted by air-water interfaces in partly saturated 3-phase systems. However, DLVO theory does not account for hydrophobic forces and thus cannot predict bacteria interaction with air-water interfaces. These deviations may be explained by the XDLVO and by hydrophobic forces.

3.7.2. XDLVO interactions

The XDLVO calculations are given in Fig. 4b. The results also predicted unfavourable attachment conditions for all cases except for *R. erythropolis* in water repellent sand (< ~2 nm), but lower energy barriers for both bacteria in the water repellent sand compared to wettable (in contrast to DLVO, Fig. 4a). The results indicated that taking acid-base forces into account mitigated energy barriers for water repellent medium rather than the wettable one. The XLDVO findings were more consistent with the BTCs, mass recovery, and inverse modeling by HYDRUS, and the previous studies in which lower energy barriers were reported for higher ionic strengths [16,51,52]. The XLDVO results still demonstrated some deviations to predict bacteria attachment or retention; i.e. the high retention of *E. coli* in the water repellent sand.

Interactions between bacteria and air-water interfaces were estimated by hydrophobic forces (Fig. 5). The hydrophobic potential energy was highly attractive for *R. erythropolis* for long distances (~435 nm) compared to *E. coli*. For the latter, the attractive potentials calculated for much smaller distances (~4 nm) with a considerably lower attractive potential than *R. erythropolis*. This supports the increase of bacteria attachment to air-water interfaces with increasing cell hydrophobicity [31]. If XDLVO is considered (Fig. 4b), the repulsive energies were mitigated where at least one hydrophobic interaction combination was present (i.e., cell-medium). This means the energy barriers for bacteria for both air-water and solid-water interfaces were moderated by attractive hydrophobic forces particularly for the short separation distances. This could explain the higher values for k_{att} for both bacteria in water repellent compared to wettable sand, no matter that attachment at liquid-air interfaces should also be present in both column systems.

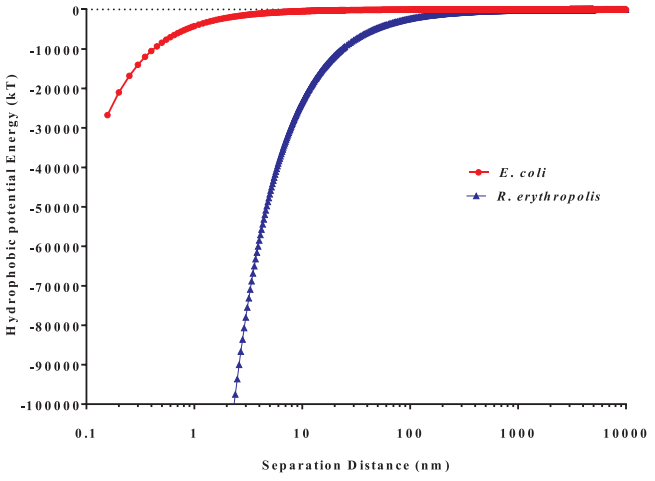

Fig. 5. Calculated hydrophobic interaction energy profiles for *Escherichia coli* (*E. coli*) and *Rhodococcus erythropolis* (*R. erythropolis*) as a function of separation distance interacting with air-water interface.

The hydrophobic interaction energies between bacteria and air-water interfaces were greater than those yielded in the solid-water interfaces (data not presented). Fig. 5 illustrates that hydrophobic *R. erythropolis* should experience greater retention than hydrophilic *E. coli*. However, in contrast to the hydrophobic profile energy, *R. erythropolis* was retained less than *E. coli* in the water repellent sand, but, slightly more in the wettable sand. Trapped air occupied a great portion of the repellent columns (Table 1). This could also increase the probability of hydrophobic-hydrophobic interaction between bacteria and air interfaces (i.e., *R. erythropolis* with water repellent sand surface or air interfaces). If only the hydrophobic interaction is considered as an adsorption mechanism, higher retention for *R. erythropolis* would be expected [16,31]. However, significantly greater retention was observed for hydrophilic *E. coli* in the water repellent sand. This result is in contrast to the hydrophilicity of *E. coli* found in this study, and by Wan and Wilson [15] and Gargiulo et al. [45] who attributed higher bacteria retention to higher cell hydrophobicity. As mentioned earlier (sections *3.1* and *3.5*), both strains are big enough to be trapped in the pore throats or film waters while *E. coli* was larger than *R. erythropolis*. Therefore, straining as film straining or retained at narrow pore structures could be more important for the observed retention of *E. coli* in water repellent sand, even for such relatively small differences. This final conclusion regarding the dominant retention mechanism concurs with other studies that outlined the importance of straining on bacteria retention in favourable and unfavorable attachment conditions [1,7,8,12,13,48]. Our study, however, also supports the assumption of the proposed hierarchy of adsorbing mechanisms for a large span of particle wettability, bacteria wettability, bacterial size, and extremely different hydraulic conditions.

Bacteria have self-regulating processes known as homeostasis that allows them to maintain their internal stability, thus guaranteeing their survival to constantly changing environmental conditions [53]. The ζ-potential results showed that *R. erythropolis* surface charges were more influenced by background KBr compared to *E. coli*. Thus, it is possible that *R. erythropolis* used such a regulating strategy during the transport through repellent sand, which had more effect than hydrophobicity and straining. Inconsistent relations between the transport of colloids and cell hydrophilicity/hydrophobicity have also been reported in various studies [16,32].

4. Conclusions

The major objective of this study was to distinguish between infiltration either into dry or wet media, and to distinguish between wettable and water repellent soil with two different bacteria differing in size and hydrophobic character.

In general, *E. coli* and *R. erythropolis* were reversibly retained in the wettable sand because of interaction energies and water flow properties. *Escherichia coli* was largely irreversibly retained compared to *R. erythropolis,* most probably due to straining in the water repellent sand. Mass balance information, numerical modeling, and calculated interaction energies suggested that retention mechanisms like straining (in terms of pore or film straining) as influenced by bacteria shape and size seem to dominate compared to attachment at liquid-solid or liquid-air interfaces. Consequently, the rate of retention was significantly

different with respect to the type of bacteria due to their size and shape. One important outcome of this study is that this holds true for each type of infiltration mode and type of soil wettability. The relative importance of either pore structure or film straining should thus be an important focus for further studies for individual pulses.

It is also evident from the results that water repellency of a particular soil is more relevant due to its impact on microscopic water distribution and corresponding effects on straining mechanisms rather than the impact of wetting properties on interaction energies, which might also affect attachment/detachment mechanisms. In short, microhydraulic processes seem to dominate compared to physico-chemical interfacial adsorption mechanisms for the selected soil-bacteria systems.

When a source of bacteria, i.e., *E. coli,* is applied to a dry wettable sandy soil, subsurface water pollution would be more probable compared with pre-wetted soil. Dry water repellent sandy soil can physically retain and filter bacteria. The distinct transport behavior of *R. erythropolis* through wettable or water repellent sands supported the conclusion that selected bacterial strains may be used for bioaugmentation practices like petroleum-affected soils, even when the vadose zone is initially dry.

Acknowledgements

This contribution was supported by the Isfahan University of Technology, Iran and the Leibniz University of Hannover, Germany. We acknowledge partial financial support of Iran National Science Foundation (INSF, no. 95848929), DFG Research Group SUBSOM, BA 1359/13-2, and German Academic Exchange Service (DAAD). We appreciate the constructive comments provided by Professor Mark Coyne from the University of Kentucky, USA and we thank Susanne K. Woche, Marc-Oliver Goebel, and Yunesh Saulick for laboratory analysis.

Appendix A. Supplementary data

Supplementary material related to this article can be found, in the online version, at doi: https://doi.org/10.1016/j.colsurfb.2018.08.044.

References

[1] J.W.A. Foppen, A. Mporokoso, J.F. Schijven, J. Contam. Hydrol. 76 (2005) 191.
[2] N. Tufenkji, M. Elimelech, Langmuir 21 (2005) 841.
[3] S.A. Bradford, S. Torkzaban, Vadose Zone J. 7 (2008) 667.
[4] S.A. Bradford, V.L. Morales, W. Zhang, R.W. Harvey, R.L. Packman, A. Mohanram, C. Welty, Crit. Rev. Environ. Sci. Technol. 43 (2013) 775.
[5] N. Sepehrnia, A.A. Mahboubi, M.R. Mosaddeghi, A.A. Safari Sinejani, G. Khodakaramian, Geoderma 217–218 (2014) 83.
[6] N. Sepehrnia, L. Memarianfard, A.A. Moosavi, J. Bachmann, G. Guggenberger, F. Rezanezhad, J. Environ. Manage. 201 (2017) 388.
[7] S.A. Bradford, J. Šimůnek, M. Bettahar, M.Th. van Genuchten, S.R. Yates, Environ. Sci. Technol. 37 (2003) 2242.
[8] S. Torkzaban, S.A. Bradford, M.Th. van Genuchten, Sh.L. Walker, J. Contam. Hydrol. 96 (2008) 113.
[9] J. Bachmann, M. Deurer, G. Arye, Vadose Zone J. 6 (2007) 436.
[10] N.J. Jarvis, Eur. J. Soil Sci. 58 (2007) 523.
[11] N. Sepehrnia, O. Fishkis, B. Huwe, J. Bachmann, J. Hydrol. Hydromech. 66 (2018) 271.
[12] S.A. Bradford, J. Šimůnek, M. Bettahar, Y.F. Tadassa, M.Th. van Genuchten, S.R. Yates, Water Resour. Res. 41 (2005) W10404.
[13] S.A. Bradford, J. Šimůnek, M. Bettahar, M.Th. van Genuchten, S.R. Yates, Water Resour. Res. 42 (2006) W12S15.
[14] J.F. Schijven, S.M. Hassanizadeh, J. Contam. Hydrol. 57 (2002) 259.
[15] J. Wan, J.L. Wilson, Water Resour. Res. 30 (1994) 11.
[16] H. Bai, N. Cochet, A. Pauss, E. Lamy, Colloids Surf. B Biointerfaces 150 (2017) 41.
[17] G.J.H. Muehl, J. Ruehlmann, M.O. Goebel, J. Bachmann, J. Soils Sediments 12 (2012) 75.
[18] W. Zhang, V. Morales, M.E. Cakmak, A.E. Salvucci, L.D. Geohring, A.G. Hay, J.Y. Parlange, T.S. Steenhuis, Environ. Sci. Technol. 44 (2010) 4965.
[19] C.H. Bolster, Sh.L. Walker, K.L. Cook, J. Environ. Qual. 35 (2006) 1018.
[20] C. Gessa, S. Deiana, Plant Soil 140 (1992) 1.
[21] J. Bachmann, A. Ellies, K.H. Hartge, J. Hydrol. 231–232 (2000) 66.
[22] Fogale, Fogale Nanotech User Manual Version 1.5. Nimes, France (2005).
[23] A. Klute, C. Dirksen, A. Klute (Ed.), Methods of Soil Analysis. Part 1. Physical and Mineralogical Methods, 2nd ed., 1986, pp. 687–732. ASA/SSSA Monograph 9(1), Madison, WI.
[24] M. Rosenberg, FEMS Microbiol. Lett. 262 (2006) 129.
[25] B.V. Derjaguin, Discus. Faraday. Soc. 18 (1954) 85.
[26] E.J.W. Verwey, J.T.G. Overbeek, Theory of the Stability of Lyophobic Colloids, Elsevier, Amsterdam, 1948 216 pp.
[27] J. Gregory, J. Colloid Interface Sci. 83 (1981) 138.
[28] R. Hogg, T.W. Healy, D.W. Fuerstenau, Trans. Faraday Soc. 62 (1966) 1638.
[29] C.J. van Oss, R.E. Giese, P.M. Costanzo, Clay Clay Miner. 38 (1990) 1511.
[30] R. Bos, H.C. van der Mei, H.J. Busscher, FEMS Microbiol. Rev. 23 (1999) 179.
[31] R.H. Yoon, D.H. Flinn, Y.I. Rabinovich, J. Colloid Interface Sci. 185 (1997) 363.
[32] A. Schäfer, P. Ustohal, H. Harms, F. Stauffer, T. Dracos, A.J.B. Zehnder, J. Contam. Hydrol. 33 (1998) 149.
[33] A.K. Guber, J.S. Karns, Y.A. Pachepsky, A.M. Sadeghi, J.S. van Kessel, T.H. Dao, Lett. Appl. Microbiol. 44 (2007) 161.
[34] E. Jawetz, J.L. Melnick, E.A. Adelberg, Medical Microbiology, 19th ed., Appleton and Lange, 2001.
[35] J. Šimůnek, M.Th. van Genuchten, Vadose Zone J. 7 (2008) 782.
[36] J.F. Schijven, J. Šimůnek, J. Contam. Hydrol. 55 (2002) 113.
[37] M.Th. van Genuchten, Soil Sci. Soc. Am. J. 44 (1980) 892.
[38] Z. Adamczyk, B. Siwek, M. Zembala, P. Belouschek, Adv. Colloid Interface Sci. 48 (1994) 151.
[39] X. Li, X. Xue, R.M. Pashley, Colloids Surf. B Biointerfaces 135 (2015) 811.
[40] F. Hamadi, H. Latrache, Colloids Surf. B Biointerfaces 65 (2008) 134.
[41] W.N. Chang, Ch.W. Liu, H.Sh. Liu, Process Biochem. 44 (2009) 955.
[44] H.H. Gerke, M.Th. van Genuchten, Water Resour. Res. 29 (1993) 305.
[45] G. Gargiulo, S.A. Bradford, J. Šimůnek, P. Ustohal, H. Vereecken, E. Klumpp, J. Contam. Hydrol. 92 (2007) 255.
[46] J.T. Crist, Y. Zevi, J.F. McCarthy, P. Baveye, J.A. Throop, T.S. Steenhuis, T.S, Vadose Zone J. 4 (2005) 184.
[47] T.A. Camesano, K.M. Unice, B.E. Logan, Colloids Surf. A Physicochem. Eng. Asp. 160 (1999) 291.
[48] J. Wan, T.K. Tokunaga, Environ. Sci. Technol. 31 (1997) 2413.
[49] C. Shen, V. Lazouskaya, H. Zhang, F. Wang, B. Li, Y. Jin, Y. Huang, Colloids Surf. A Physicochem. Eng. Aspects 410 (2012) 98–110.
[50] C. Shen, F. Wang, B. Li, Y. Yan Jin, L.P. Wang, H. Huang, Langmuir 28 (2012) 14681.
[51] J.J. Johanson, L. Feriancikova, A. Banerjee, D.A. Saffarini, L. Wang, J. Li, T.J. Grundl, Sh. Xu, Colloids Surf. B Biointerfaces 123 (2014) 439.
[52] C. Shen, L.P. Wang, B. Li, Y. Huang, Y. Jin, Vadose Zone J. 11 (2011) 162.
[53] S. Taheri-Araghi, S. Bradde, J.T. Sauls, N.S. Hill, A.P. Levin, J. Paulsson, M. Vergassola, S. Jun, Curr. Biol. 25 (2015) 385.